Constraints on the Nucleon Strange Form Factors at $Q^2 \sim 0.1\,\mathrm{GeV}^2$

K. A. Aniol,[1] D. S. Armstrong,[2] T. Averett,[2] H. Benaoum,[3] P. Y. Bertin,[4] E. Burtin,[5] J. Cahoon,[6] G. D. Cates,[7] C. C. Chang,[8] Y.-C. Chao,[9] J.-P. Chen,[9] Seonho Choi,[10] E. Chudakov,[9] B. Craver,[7] F. Cusanno,[11] P. Decowski,[12] D. Deepa,[13] C. Ferdi,[4] R. J. Feuerbach,[9] J. M. Finn,[2] S. Frullani,[11] K. Fuoti,[6] F. Garibaldi,[11] R. Gilman,[14,9] A. Glamazdin,[15] V. Gorbenko,[15] J. M. Grames,[9] J. Hansknecht,[9] D. W. Higinbotham,[9] R. Holmes,[3] T. Holmstrom,[2] T. B. Humensky,[16] H. Ibrahim,[13] C. W. de Jager,[9] X. Jiang,[14] L. J. Kaufman,[6] A. Kelleher,[2] A. Kolarkar,[17] S. Kowalski,[18] K. S. Kumar,[6] D. Lambert,[12] P. LaViolette,[6] J. LeRose,[9] D. Lhuillier,[5] N. Liyanage,[7] D. J. Margaziotis,[1] M. Mazouz,[19] K. McCormick,[14] D. G. Meekins,[9] Z.-E. Meziani,[10] R. Michaels,[9] B. Moffit,[2] P. Monaghan,[18] C. Munoz-Camacho,[5] S. Nanda,[9] V. Nelyubin,[7,20] D. Neyret,[5] K. D. Paschke,[6] M. Poelker,[9] R. Pomatsalyuk,[15] Y. Qiang,[18] B. Reitz,[9] J. Roche,[9] A. Saha,[9] J. Singh,[7] R. Snyder,[7] P. A. Souder,[3] R. Subedi,[21] R. Suleiman,[18] V. Sulkosky,[2] W. A. Tobias,[7] G. M. Urciuoli,[11] A. Vacheret,[5] E. Voutier,[19] K. Wang,[7] R. Wilson,[22] B. Wojtsekhowski,[9] and X. Zheng[23]

(The HAPPEX Collaboration)

[1] *California State University, Los Angeles, Los Angeles, California 90032, USA*
[2] *College of William and Mary, Williamsburg, Virginia 23187, USA*
[3] *Syracuse University, Syracuse, New York 13244, USA*
[4] *Université Blaise Pascal/CNRS-IN2P3, F-63177 Aubière, France*
[5] *CEA Saclay, DAPNIA/SPhN, F-91191 Gif-sur-Yvette, France*
[6] *University of Massachusetts Amherst, Amherst, Massachusetts 01003, USA*
[7] *University of Virginia, Charlottesville, Virginia 22904, USA*
[8] *University of Maryland, College Park, Maryland 20742, USA*
[9] *Thomas Jefferson National Accelerator Facility, Newport News, Virginia 23606, USA*
[10] *Temple University, Philadelphia, Pennsylvania 19122, USA*
[11] *INFN, Sezione Sanità, 00161 Roma, Italy*
[12] *Smith College, Northampton, Massachusetts 01063, USA*
[13] *Old Dominion University, Norfolk, Virginia 23508, USA*
[14] *Rutgers, The State University of New Jersey, Piscataway, New Jersey 08855, USA*
[15] *Kharkov Institute of Physics and Technology, Kharkov 310108, Ukraine*
[16] *University of Chicago, Chicago, Illinois 60637, USA*
[17] *University of Kentucky, Lexington, Kentucky 40506, USA*
[18] *Massachusetts Institute of Technology, Cambridge, Massachusetts 02139, USA*
[19] *Laboratoire de Physique Subatomique et de Cosmologie, 38026 Grenoble, France*
[20] *St.Petersburg Nuclear Physics Institute of Russian Academy of Science, Gatchina, 188350, Russia*
[21] *Kent State University, Kent, Ohio 44242, USA*
[22] *Harvard University, Cambridge, Massachusetts 02138, USA*
[23] *Argonne National Laboratory, Argonne, Illinois, 60439, USA*

(Dated: June 7, 2005)

We report the most precise measurement to date of a parity-violating asymmetry in elastic electron-proton scattering. The measurement was carried out with a beam energy of 3.03 GeV and a scattering angle $\langle\theta_{lab}\rangle = 6.0^\circ$, with the result $A_{\mathrm{PV}} = (-1.14 \pm 0.24\ (\mathrm{stat}) \pm 0.06\ (\mathrm{syst})) \times 10^{-6}$. From this we extract, at $Q^2 = 0.099\,\mathrm{GeV}^2$, the strange form factor combination $G_E^s + 0.080\,G_M^s = 0.030 \pm 0.025\,(\mathrm{stat}) \pm 0.006\,(\mathrm{syst}) \pm 0.012\,(\mathrm{FF})$ where the first two errors are experimental and the last error is due to the uncertainty in the neutron electromagnetic form factor. The measurement significantly improves existing constraints on G_E^s and G_M^s at $Q^2 \sim 0.1\,\mathrm{GeV}^2$. A consistent picture emerges from all measurements at this Q^2. A combined fit shows that G_E^s is consistent with zero while G_M^s prefers positive values though $G_E^s = G_M^s = 0$ is compatible with the data at 95% C.L.

PACS numbers: 13.60.Fz, 11.30.Er, 13.40.Gp, 14.20.Dh

The nucleon is a bound state of three valence quarks, but a rich structure is evident when it is probed over a wide range of length scales in scattering experiments. In one class of measurements, elastic lepton-nucleon electromagnetic scattering is used to measure electric and magnetic form factors, which are functions of the 4-momentum transfer Q^2 and carry information on the nucleon charge and magnetization distributions.

A "sea" of virtual quark-antiquark pairs of the three light (up, down and strange) flavors and gluons surrounds each constituent quark. One way to probe the sea is to investigate whether strange quarks contribute to the static properties of the nucleon. Establishing a nontrivial role for the sea would provide new insight into nonperturbative dynamics of the strong interactions.

Weak neutral current (WNC) elastic scattering, me-

diated by the Z^0 boson, measures form factors that are sensitive to a different linear combination of the three light quark distributions. When combined with proton and neutron electromagnetic form factor data and assuming isospin symmetry, the strange electric and magnetic form factors G_E^s and G_M^s can be isolated, thus accessing the nucleon's strange quark charge and magnetization distributions [1].

Parity-violating electron scattering is a particularly clean experimental technique to extract the WNC amplitude [2, 3]. Such experiments involve the scattering of longitudinally polarized electrons from unpolarized targets, allowing the determination of a parity-violating asymmetry $A_{\rm PV} \equiv (\sigma_R - \sigma_L)/(\sigma_R + \sigma_L)$, where $\sigma_{R(L)}$ is the cross section for incident right(left)-handed electrons. $A_{\rm PV}$ arises from the interference of the weak and electromagnetic amplitudes [4]. Typical asymmetries are small, ranging from 0.1 to 100 parts per million (ppm).

Three experiments have published $A_{\rm PV}$ measurements in elastic electron-proton scattering. The SAMPLE result [5] at backward angle constrained G_M^s at $Q^2 \sim 0.1\,{\rm GeV}^2$. The HAPPEX [6] and A4 [7, 8] results at forward angle constrained a linear combination of G_E^s and G_M^s in the range $0.1 < Q^2 < 0.5\,{\rm GeV}^2$. While no measurement independently indicates a significant strange form factor contribution, the A4 measurement at $Q^2 = 0.108\,{\rm GeV}^2$ is 2σ away from the theoretical expectation neglecting strange quarks [8].

In this paper, we report a new measurement of $A_{\rm PV}$ in elastic electron-proton scattering at $Q^2 \sim 0.1\,{\rm GeV}^2$. This first result from experiment E99-115 at the Thomas Jefferson National Accelerator Facility (JLab) has achieved the best precision on $A_{\rm PV}$ in electron-nucleon scattering. We describe the experimental technique below, which has several features that allow for very small overall statistical and systematic uncertainty. The ultimate goal of the experiment is to reach a precision $\delta(A_{\rm PV}) \sim 0.1$ ppm.

The experiment is situated in Hall A at JLab. A 35 μA continuous-wave beam of longitudinally polarized 3.03 GeV electrons is incident on a 20 cm long liquid hydrogen target. Scattered electrons are focused by twin spectrometers onto total-absorption detectors situated in heavily-shielded detector huts, creating a clean separation between elastically scattered electrons and inelastic backgrounds. The spectrometers are arranged to create an approximately left-right symmetric acceptance.

Two separate detector segments in each spectrometer arm cover the full flux of elastically scattered electrons, for a total of 4 detector photomultiplier tubes (PMTs). The PMT response is integrated; the detector elements and the associated electronics are designed to accept an elastic flux rate of ~ 120 MHz at full design luminosity.

The experimental configuration is similar to the previous measurement of $A_{\rm PV}$ at $Q^2 \sim 0.5$ GeV^2 [6]. The new configuration, including the addition of septum magnets to accept scattered electrons with $\langle\theta_{lab}\rangle \sim 6^\circ$, is described in more detail in the paper reporting the $A_{\rm PV}$ result with a ^{4}He target [9].

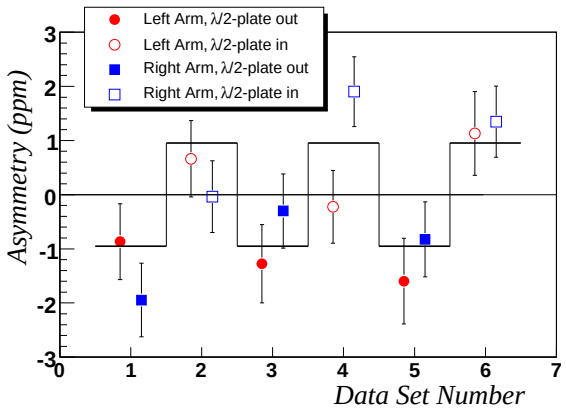

FIG. 1: $A_{\rm raw}$ for all data, grouped by $\lambda/2$-plate state in sequential samples. The circles and squares represent the average of the 2 PMT channels in each spectrometer arm.

The helicity of the polarized electron beam is set every 33.3 ms; each of these periods of constant helicity will be referred to as a "window." The helicity sequence is structured as pairs of windows with opposite helicity ("window pairs"), with the helicity of the first window selected pseudo-randomly. The integrated response of the detector PMTs, beam current monitors, and beam position monitors is digitized and recorded into the data stream for each window.

The data sample consists of roughly 11 million helicity-window pairs. Loose requirements are imposed on beam quality which remove periods of current, position, or energy instability from the final data set. However, no helicity-dependent cuts are applied. After applying selection criteria, 9.96×10^6 window pairs remain for further analysis.

The right-left asymmetry in the integrated detector response, normalized to the average beam current for each window, is computed for each window pair and then corrected for fluctuations in the beam trajectory to form the raw asymmetry $A_{\rm raw}$. The first order dependence on five correlated beam parameters (energy and horizontal and vertical position and angle) is removed by two independent analysis methods; the numerical difference between the two results is negligible compared to the final statistical uncertainty.

The $A_{\rm raw}$ window-pair distribution has an RMS of ~ 620 ppm. Non-Gaussian tails are negligible over more than 4 orders of magnitude. This demonstrates that the distribution is dominated by the counting statistics of an elastically scattered electron rate of $\sim$ 40 MHz. Contributions to the fluctuations from background, electron beam, electronic noise or target density are negligible.

The cumulative correction for $A_{\rm raw}$ due to helicity-correlated differences in electron beam parameters is

-0.079 ± 0.032 ppm. This correction is small compared to the statistical error on $A_{\rm raw}$ due to several important factors. First, careful attention is given to the design and configuration of the laser optics in the polarized source to reduce helicity-correlated beam asymmetries to a manageable level. Over the duration of data collection, the cumulative helicity-correlated asymmetries in the electron beam are 0.022 ppm in energy, 8 nm in position, and 4 nrad in angle.

Additionally, the asymmetry averaged over all PMTs is quite insensitive to the beam trajectory due to the symmetric detector configuration. The largest correction of -0.130 ppm is from the beam monitor that is predominantly sensitive to the helicity-correlated beam energy asymmetry. The systematic error in the correction is estimated by studying residual correlations of beam asymmetries with the responses of individual PMTs, which are significantly more sensitive to the beam trajectory.

The effect of charge normalization is a 2.6 ppm correction to the detector-response asymmetry. Dedicated calibration runs are used to constrain the relative alinearity between the beam monitors and the detectors ($< 0.2\%$) and the absolute alinearity of the detector PMTs ($< 1\%$). No alinearity correction to $A_{\rm raw}$ is applied, while an uncertainty of 0.015 ppm is assigned.

A half-wave ($\lambda/2$) plate is periodically inserted into the laser optical path, passively reversing the sign of the electron beam polarization. Roughly equal statistics are thus accumulated with opposite signs for the measured asymmetry, which suppresses many systematic effects. Figure 1 shows $A_{\rm raw}$ for all data, averaged over the 2 PMT channels in each spectrometer, grouped by $\lambda/2$-plate state and divided into 6 sequential samples.

The physics asymmetry $A_{\rm PV}$ is formed from $A_{\rm raw}$ by correcting for beam polarization, backgrounds, and finite acceptance:

$$A_{\rm PV} = \frac{K}{P_b}\frac{A_{\rm raw} - \sum_i A_i f_i}{1 - \sum_i f_i} \qquad (1)$$

where P_b is the beam polarization, f_i are background fractions and A_i the associated background asymmetries, and K accounts for the range of kinematic acceptance.

The beam polarization measured by the Hall A Compton polarimeter [10] is determined to be $P_b = 0.813 \pm 0.016$, averaged over the duration of the run. The result is consistent, within systematic uncertainties, with dedicated polarization measurements using Møller scattering in Hall A and Mott scattering in the low-energy injector.

The average Q^2 is determined to be $\langle Q^2 \rangle = 0.099 \pm 0.001\,{\rm GeV}^2$ by dedicated low-current runs; the uncertainty in this value contributes to the systematic error of the asymmetry. The acceptance correction to account for the non-linear dependence of the asymmetry with Q^2 is computed, using a Monte Carlo simulation, to be $K = 0.976 \pm 0.006$.

Correction (ppm)	
Target windows	0.006 ± 0.016
Rescatter	0.000 ± 0.031
Beam Asyms.	-0.079 ± 0.032
Alinearity	0.000 ± 0.015

Normalization Factors	
Polarization P_b	0.813 ± 0.016
Acceptance K	0.976 ± 0.006
Q^2 Scale	1.000 ± 0.010

TABLE I: Corrections to $A_{\rm raw}$ and systematic uncertainties.

Largely due to the excellent hardware resolution of the spectrometers ($\delta p/p < 0.1\%$), the total dilution to the PMT response from all background sources is less than 1%. The largest contribution of 0.9% comes from the aluminum windows of the cryogenic target. The asymmetry of the background is of the same sign and similar magnitude to that of $A_{\rm PV}$ from elastic scattering off hydrogen, which reduces its effect on the measurement.

While inelastic scattering backgrounds do not directly reach the detectors, dedicated runs are used to estimate the contribution from charged particles which rescatter inside the spectrometers. Rates in the detectors are studied as the central spectrometer momentum is varied. Individual scattered electrons are tracked, using drift chambers at low beam currents, to determine the location of rescattering in the spectrometer. From these studies, an upper limit on $A_{\rm PV}$ due to possible rescattering from polarized iron or unpolarized material is determined to be 0.031 ppm.

The corrections are summarized in Table I. After all corrections, the result at $Q^2 = 0.099\,{\rm GeV}^2$ is

$$A_{\rm PV} = -1.14 \pm 0.24\ ({\rm stat}) \pm 0.06\ ({\rm syst})\ {\rm ppm}. \qquad (2)$$

Additional details of this analysis are given in [9].

This parity-violating asymmetry is given in the standard model by:

$$A_{\rm PV} = -\frac{G_F Q^2}{4\pi\alpha\sqrt{2}} \times \left\{ (1+R_V^p)(1-4\sin^2\theta_W) - (1+R_V^n)\frac{\epsilon G_E^{\gamma p} G_E^{\gamma n} + \tau G_M^{\gamma p} G_M^{\gamma n}}{\epsilon (G_E^{\gamma p})^2 + \tau (G_M^{\gamma p})^2} - (1-R_V^{(0)})\frac{\epsilon G_E^{\gamma p} G_E^{s} + \tau G_M^{\gamma p} G_M^{s}}{\epsilon (G_E^{\gamma p})^2 + \tau (G_M^{\gamma p})^2} \right.$$
$$\left. - \frac{(1-4\sin^2\theta_W)\,\epsilon'\, G_M^{\gamma p}}{\epsilon (G_E^{\gamma p})^2 + \tau (G_M^{\gamma p})^2} \left[-2\,(1+R_A^{T=1})\, G_A^{T=1} + (\sqrt{3} R_A^{T=0})\, G_A^{T=0} \right] \right\} \quad (3)$$

where $G_{E(M)}^{\gamma p(n)}$ are the proton (neutron) electric (magnetic) form-factors, $G_A^{T=1(0)}$ is the isovector (isoscalar) proton axial form factor, G_F is the Fermi constant, α is the fine structure constant, and θ_W is the electroweak mixing angle. All form factors are functions of Q^2, and $\epsilon = 0.994$, $\tau = 0.028$, $\epsilon' = 0.018$ are kinematic quantities. The $R_{V,A}$ factors parametrize the electroweak radiative corrections of the neutral weak current [3]. All the vector corrections [3] and the axial corrections [11] are converted to their ($\overline{MS}$) values with $\sin^2\theta_W \equiv \sin^2\hat{\theta}_W(M_Z) = 0.23120(15)$ [12]. Corrections due to purely electromagnetic radiative corrections are negligible due to the small momentum acceptance ($\delta p/p < 3\%$) and the spin independence of soft photon emission [13].

The values for the electromagnetic form factors $G_{E(M)}^{\gamma p(n)}$ are taken from a recently published phenomenological fit to world data at low Q^2 [14], with uncertainties in each value based on error bars of data near $Q^2 = 0.1\,{\rm GeV}^2$. The values (and relative uncertainty) used are: $G_E^p = 0.754$ (2.5%), $G_M^p = 2.144$ (1.5%), $G_E^n = 0.035$ (30.0%), and $G_M^n = -1.447$ (1.5%). The contribution from axial form factors is calculated to be 0.026 ± 0.008 ppm at these kinematics.

At the central kinematics, $A_{\rm PV}$ is estimated ($G^s = 0$) to be $A_{\rm PV}^{(s=0)} = -1.43 \pm 0.11\,({\rm FF})$ ppm where the error comes mainly from the uncertainty in G_E^n. We thus extract a measurement of the combination of strange form-factors: $G_E^s + 0.080\,G_M^s = 0.030 \pm 0.025\,({\rm stat}) \pm 0.006\,({\rm syst}) \pm 0.012\,({\rm FF})$ at $Q^2 = 0.099\,{\rm GeV}^2$.

Figure 2 shows the combination $G_E^s + \eta\, G_M^s$ from our measurement, along with the three published forward angle $A_{\rm PV}$ measurements using a hydrogen target. Here, η, which is different for each measurement plotted, increases with Q^2 and ranges from 0.08 to 0.4 in the region of interest. It can be seen that, while each independent measurement does not show a statistically significant non-zero $G_E^s + \eta\, G_M^s$, the data suggests a positive contribution. Additional data on $A_{\rm PV}$ in forward-angle scattering from hydrogen in the range $Q^2 = 0.12\,{\rm GeV}^2$ to $Q^2 = 1.0\,{\rm GeV}^2$ from the G0 collaboration will be available soon [15].

A combined fit of all the measurements at $Q^2 \sim 0.1\,{\rm GeV}^2$ is used to obtain a constraint in the G_E^s-G_M^s plane. Figure 3 shows the four measurements, as well as the 95% allowed contour from a combined fit. The combined best fit values are $G_E^s = -0.01 \pm 0.03$ and $G_M^s = +0.55 \pm 0.28$. While this fit favors positive values for G_M^s, the origin ($G^s = 0$) is still allowed at the 95% C.L. Figure 3 also shows results from various theoretical calculations [16]-[22].

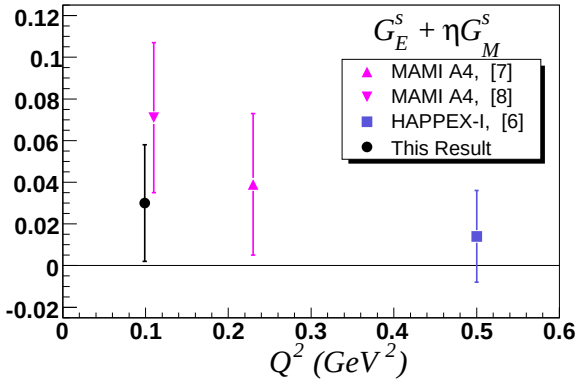

FIG. 2: Constraint on $G_E^s(Q^2)+\eta(Q^2)\,G_M^s(Q^2)$ from the measurement. Also shown are the three published $A_{\rm PV}$ measurements in elastic electron-proton scattering at forward angle.

In conclusion, we report a precise measurement of $A_{\rm PV}$ in elastic electron-proton scattering at $Q^2 = 0.099\,{\rm GeV}^2$. This has resulted in improved constraints on the strange form factors at $Q^2 \sim 0.1\,{\rm GeV}^2$. The HAPPEX measurements at $Q^2 \sim 0.1\,{\rm GeV}^2$ from both ^{1}H and ^{4}He targets will be improved by a factor of 2 to 3 in precision in a new run scheduled for Fall 2005. Given the currently allowed region in Fig. 3, such precision has the potential to dramatically impact our understanding of the role of strange quarks in the nucleon.

We wish to thank the entire staff of JLab for their efforts to develop and maintain the polarized beam and the experimental apparatus. This work was supported by DOE contract DE-AC05-84ER40150 Modification No. M175, under which the Southeastern Universities Research Association (SURA) operates JLab, and by the Department of Energy, the National Science Foundation, the INFN (Italy), the Natural Sciences and Engineering Research Council of Canada, and the Commissariat à l'Énergie Atomique (France).

[1] D. B. Kaplan and A. Manohar, Nucl. Phys. B **310**, 527 (1988).

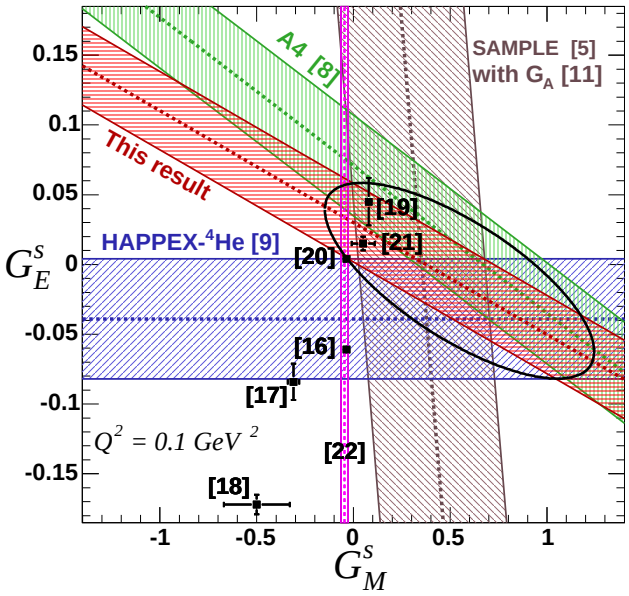

FIG. 3: The four $A_{\rm PV}$ measurements at $Q^2 \sim 0.1\,{\rm GeV}^2$ are shown, with shaded bands representing the 1-sigma combined statistical and systematic uncertainty. Also shown is the combined 95% C.L. ellipse from all four measurements. The black squares and narrow vertical band represent various theoretical calculations ([16]-[22]).

[2] R. D. McKeown, Phys. Lett. B **219**, 140 (1989).
[3] M. J. Musolf *et al.*, Phys. Rep. **239**, 1 (1994).
[4] Ya. B. Zel'dovich, Sov. Phys. JETP, **36**, 964 (1959).
[5] D. T. Spayde *et al.*, Phys. Lett. B **583**, 79 (2004).
[6] K. A. Aniol *et al.*, Phys. Lett. B **509**, 211 (2001); K. A. Aniol *et. al.*, Phys. Rev. C **69**, 065501 (2004).
[7] F. E. Maas *et al.*, Phys. Rev. Lett. **93**, 022002 (2004).
[8] F. E. Maas *et al.*, Phys. Rev. Lett. **94**, 152001 (2005).
[9] K. A. Aniol *et al.* nucl-ex/0506010.
[10] S. Escoffier *et al.*, physics/0504195.
[11] S.-L. Zhu *et al.*, Phys. Rev. D **62**, 033008 (2000).
[12] J. Erler and P. Langacker, Phys. Lett. B **592**, 114 (2004).
[13] L. C. Maximon and W. C. Parke, Phys. Rev. C **61**, 045502 (2000).
[14] J. Friedrich and Th. Walcher, Eur. Phys. J. A **17**, 607 (2003).
[15] D. H. Beck *et al.*, TJNAF Experiment E00-006.
[16] N. W. Park and H. Weigel, Nucl. Phys. A **451**, 453 (1992).
[17] H. W. Hammer, U. G. Meissner, and D. Drechsel, Phys. Lett. B **367**, 323 (1996).
[18] H.-W. Hammer and M. J. Ramsey-Musolf, Phys. Rev. C **60**, 045204 (1999).
[19] A. Silva *et al.*, Phys. Rev. D **65**, 014015 (2001).
[20] V. Lyubovitskij *et al.*, Phys. Rev. C **66**, 055204 (2002).
[21] R. Lewis *et al.*, Phys. Rev. D **67**, 013003 (2003).
[22] D. B. Leinweber *et al.*, hep-lat/0406002.